

Creatine kinase in energy metabolic signaling in muscle

Olav Kongas^{*}
Institute for Cardiovascular Research
Free University Amsterdam
Van der Boechorststraat 7
1081 BT, Amsterdam, the Netherlands
ok@mito.physiol.med.vu.nl

Johannes H.G.M. van Beek
Faculty of Biology, Free University Amsterdam
De Boelelaan 1087
1081 HV, Amsterdam, the Netherlands
hvanbeek@bio.vu.nl

ABSTRACT

There has been much debate on the mechanism of regulation of mitochondrial ATP synthesis to balance ATP consumption during changing cardiac workloads. A key role of creatine kinase (CK) isoenzymes in this regulation of oxidative phosphorylation and in intracellular energy transport had been proposed, but has in the mean time been disputed for many years. It was hypothesized that high-energy phosphoryl groups are obligatorily transferred via CK; this is termed the phosphocreatine shuttle. The other important role ascribed to the CK system is its ability to buffer ADP concentration in cytosol near sites of ATP hydrolysis.

Almost all of the experiments to determine the role of CK had been done in the steady state, but recently the dynamic response of oxidative phosphorylation to quick changes in cytosolic ATP hydrolysis has been assessed at various levels of inhibition of CK. Steady state models of CK function in energy transfer existed but were unable to explain the dynamic response with CK inhibited.

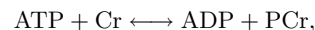
The aim of this study was to explain the mode of functioning of the CK system in heart, and in particular the role of different CK isoenzymes in the dynamic response to workload steps. For this purpose we used a mathematical model of cardiac muscle cell energy metabolism containing the kinetics of the key processes of energy production, consumption and transfer pathways. The model underscores that CK plays indeed a dual role in the cardiac cells. The buffering role of CK system is due to the activity of myofibrillar CK (MMCK) while the energy transfer role depends on the activity of mitochondrial CK (MiCK). We propose that this may lead to the differences in regulation mechanisms and energy transfer modes in species with relatively low MiCK activity such as rabbit in comparison with species with high MiCK activity such as rat.

The model needed modification to explain the new type of experimental data on the dynamic response of the mitochondria. We submit that building a Virtual Muscle Cell is not possible without continuous experimental tests to improve the model. In close interaction with experiments we are developing a model for muscle energy metabolism and transport mediated by the creatine kinase isoforms which now already can explain many different types of experiments.

^{*}On the leave from Institute of Cybernetics at Tallinn Technical University, Akadeemia 21, 12618 Tallinn, Estonia

1. INTRODUCTION

ATP, a major carrier of readily available energy in cells, is synthesized in the mitochondria and its major use in muscle is for myofibrillar contraction and ion pumping. Phosphocreatine (PCr) is known to be another abundant energy carrier in normal muscle cells. The transport of energy from mitochondria to myofibrils is a process involving intermediate energy carriers, several enzymatic reactions, and diffusion through various structures in the cell. The major part of the energy-carrying phosphate groups may leave the mitochondria in the form of PCr and not as ATP. This is possible because of the creatine kinase (CK) reaction



where Cr is creatine. The mitochondrial CK isoform (MiCK) produces usually PCr while the major myofibrillar isoform (MMCK) converts it back to ATP. Such transfer of energy has been termed the *phosphocreatine shuttle* [2]. The PCr shuttle facilitates energy transfer by providing a parallel pathway to ATP diffusion. The CK system has also another important function in muscle cells — energy buffering. In skeletal muscle the fluctuation of PCr follows closely the force generation during a contraction cycle while ATP remains constant [4]. Such strong buffering is essential to keep intracellular ATP high and ADP low.

During the last decade, a technique to measure the response time, t_{mito} , of mitochondrial oxygen consumption to rapid workload steps in perfused hearts has been developed (see [23] for a review). Recently, the technique was used to assess t_{mito} of rabbit hearts after a graded inhibition of the CK [10]. It turned out that the inhibition of CK led to shortening of t_{mito} meaning faster signal transduction. This effect might be ascribed to the impaired buffering capacity of the CK system. Also, this result indicates that the functioning of the PCr shuttle is not obligatory to regulate the energy production and sustain the energy transfer at low or moderate workloads. Under stress conditions, however, the impaired CK activity prevents the perfused hearts to express the full dynamic range of myocardial contractile performance [9]. Apparently, the mode of functioning of CK isoenzymes and their role in energy transfer and buffering depends on the working conditions.

The aim of this study was to determine the mode of functioning of the CK system in heart. We developed a simple mathematical model of an energy production, transfer, and

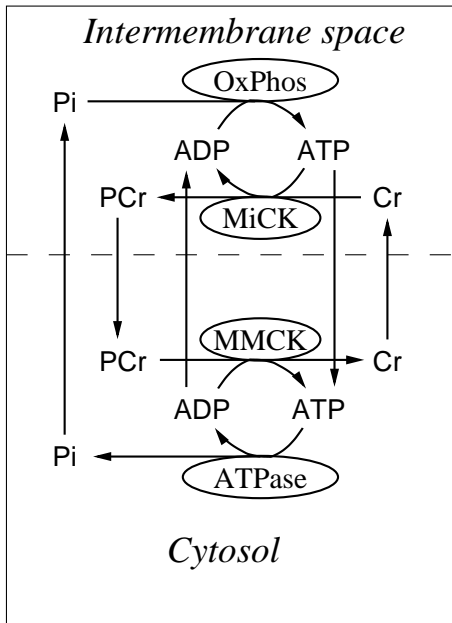


Figure 1: Schematic representation of the model. The model consists of two compartments: the cytosol and the intermembrane space (IMS). The compartments are separated by a partly permeable diffusion barrier; the vertical arrows crossing the barrier show the diffusional fluxes. The metabolites involved in the model are ATP, ADP, PCr (phosphocreatine), Cr (creatine), and Pi (inorganic phosphate). The reactions: ATP production (OxPhos), ATP consumption (ATPase), mitochondrial and myofibrillar creatine kinases (MiCK and MMCK, resp.).

consumption and analyzed the roles of different CK isoenzymes in the dynamic response to workload transitions.

2. THE MODEL

2.1 Construction of the model

To analyze the mitochondrial response time we constructed a very simple mathematical model of a cardiac cell energy metabolism containing only the kinetics of CK isoenzymes in mitochondrial and cytosolic compartments (MiCK and MMCK, respectively), Michaelis-Menten-type kinetics of ATP synthesis and ATP hydrolysis rate as input parameters (see Figure 1). The model equations are given in Appendix. This model is a simplified version of the much more extensive model that we have developed previously [24]. Next we give a brief description of the original model, the steps taken to simplify it and a discussion of the influence of each simplification.

In the original model, the compartmentalized energy transfer from a mitochondrion to a myofibril was simulated by a spatially inhomogeneous (distributed) reaction-diffusion processes. The model considered the reactions of three main compartments: the myofibril together with the myoplasm, the mitochondrial intermembrane space (IMS), and the mitochondrial matrix space. The metabolites described by the

model in the myofibrils and IMS were ATP, ADP, AMP, phosphocreatine (PCr), creatine (Cr), and inorganic phosphate (Pi). All these metabolites could diffuse between the cytosolic and IMS compartments, where the metabolites were involved in the CK and adenylate kinase (AK) reactions. The ATP was hydrolyzed in the myofibrils. In the IMS, the mitochondrial CK (MiCK) reaction was integrated with the adenine nucleotide translocase (ANT) reaction via strong coupling between these enzymes. The model described also the kinetics of respiratory complexes (producing protonmotive force), membrane leak of protons, mitochondrial phosphate carrier and ATP synthase.

We simplified the above model by the following steps. First, we dropped the coupling between the MiCK and ANT. This was probably the most critical simplification. However, it is justified because the coupling effect is minimal at high ATP values for rabbit heart mitochondria [7] and removing the coupling did not affect the simulation results considerably. Second, since mitochondria respond to changes of ADP and Pi in their immediate environment very rapidly, we did not need such a detailed description of the mitochondrial processes. As ADP and Pi, but not ATP, are changed considerably in our simulations, sufficient similarity with the behavior of the original model was obtained using the Michaelis-Menten-type kinetics of ATP synthesis as a function of ADP_i and Pi_i (IMS concentrations of ADP and Pi, respectively). Third, we lumped all the diffusion resistances together between the cytosol and the IMS, including the mitochondrial outer membrane resistance, the latter being substantial according to Saks.et.al [18]. Fourth, we dropped the AK kinetics and AMP from the model. It turned out that the last two steps had virtually no influence on the results. However, it is relevant to keep the full kinetics for both MMCK and MiCK isoforms in the model, because our simulations involved conditions where reactions of one or both of these isoforms were strongly out of equilibrium.

The simplified model has inherited from the original model the following properties. First, for low and moderate workloads, the ATP and PCr levels remain practically constant. Second, energy transfer occurs mostly via the PCr shuttle. Third, at moderate workloads, the PCr level drops when CK is inhibited. For more thorough discussion on these properties see [24]. Thus, the simplified model reproduced the behavior of the extensive model on these points.

2.2 Numerical procedures

Figure 2 shows a schematic representation of the response of ATP production to a step of workload for both steady and oscillating workloads. For steady workload, t_{mito} was calculated in our model as follows. After stepwise increase of workload from V_1 to V_2 at time $t = 0$, the system was integrated until the transients vanished ($t = T$). Then the area between the solid and dashed line was computed for the range $0 \leq t \leq T$ and divided by the step size $V_2 - V_1$ yielding t_{mito} . This procedure corresponds to determining the first statistical central moment of the impulse response function of a linear system, and would yield the time constant in cases where the response is monoexponential [15].

For oscillating workload, the average level of workload was stepwise increased from V_1 to V_2 at $t = 0$. After the tran-

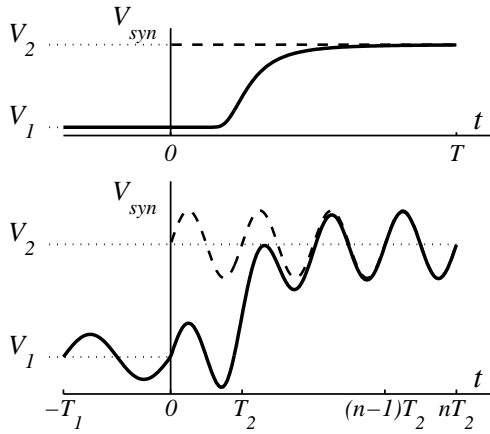


Figure 2: Schematic representation of the response of ATP synthesis to step of workload for steady (upper panel) and oscillating (lower panel) workloads. For both types of workloads, the area between the dashed and solid lines was computed in the range from $t = 0$ (workload step applied) till the transients were vanished. Normalizing this area with the step size $V_2 - V_1$ yielded the response time t_{mito} . See text for details.

sients vanished, the last period of V_{syn} in $(n-1)T_2 \leq t \leq nT_2$ was repeatedly projected back as depicted by the dashed curve in the lower panel. Then the area between the solid and dashed lines was computed for the range $0 \leq t \leq nT_2$ and divided by the step size $V_2 - V_1$ yielding t_{mito} . Note that this procedure is suitable for computing the response times when the oscillation periods before and after the step differ, i.e., $T_1 \neq T_2$.

The model equations were solved by a backward differentiation formula that is able to treat stiff equations, using the DVODE package. To fit experimental data, the model parameters were optimized by modified Levenberg-Marquardt algorithm, using the LMDIF least squares solver. To find the areas needed for t_{mito} calculations (see previous paragraph), Simpson' rule was used.

3. RESULTS

In our simulations we varied the activity of the CK system. The results are presented with respect to the relative activity of creatine kinase, V_{CK} , where $V_{CK} = 1$ corresponds to normal MiCK and MMCK activities in rabbit heart, 1.0 and 5.7 IU/mgdw, respectively [12, 16] at $T = 25^\circ\text{C}$. We simulate the processes at $T = 37^\circ\text{C}$. We present most of our results for $V_{CK} = 0 - 3$ to include the range of MiCK activities relevant for other species such as rat which has higher mitochondrial CK activity than rabbit. The baseline workload was set to $500\mu\text{M/s}$ of ATP consumption (0.101 IU/mgdw). All the fluxes given in $\mu\text{M/s}$ are calculated with respect to the total cell volume to make the fluxes in different compartments comparable.

3.1 Metabolite concentrations and fluxes

Figure 3 shows the concentrations of some cytosolic metabolites before and after the workload step from baseline to 40%

above the baseline. We have not shown the concentrations of Cr and ATP, because they can be determined from the creatine and adenine nucleotide moieties conservation, respectively. The diffusion barrier between the cytosolic and intermembrane space (IMS) compartments leads to large relative differences between the cytosolic and IMS values only for ADP (denoted as ADP_i in IMS). Note that ADP_i decreases in response to workload step for $V_{CK} > 1$.

Figure 4 shows the relative fluxes of high energy phosphates from mitochondria. The sum of these fluxes equals the baseline ATP consumption. The fluxes are equal to each other at $V_{CK} = 0.37$. This figure demonstrates the activation of the PCr shuttle if the CK system is activated. The activation is further illustrated in Figure 5 which shows the net and forward (PCr production) fluxes through the MiCK. Because the MMCK activity is about 6 times higher than that of MiCK, it reaches its equilibrium at much lower V_{CK} values. This demonstrates the different modes of functioning of the MM versus the mitochondrial CK isoenzymes in the PCr shuttle. In addition, this shows that the activity of the PCr shuttle is controlled by the activity of MiCK.

3.2 Mitochondrial response times

The mitochondrial response time, t_{mito} , depends on the chosen workload step and the baseline. According to simulations, the higher the baseline and the larger the step, the longer the response time (not shown). Our baseline was chosen to be one ninth of the maximal mitochondrial ATP synthesis capacity. As the response time is nearly constant for small workload steps, we used here a step with an amplitude of $1/1000$ of the baseline. The results for steps as large as $1/4$ of the baseline were very close to those presented here.

Figure 6 demonstrates the unimodal dependence of t_{mito} as a function of V_{CK} in our model. This property is robust: the height and exact location of the peak depend on a set of chosen parameters, but the initial increase and a decrease thereafter are persistent properties. The peak coincides with the activation of the backward flux through MiCK. The peak occurs at $V_{CK} = 0.33$. At that point, the ratio of backward and forward fluxes through the MiCK is 0.09.

To analyze the influence of the different CK isoenzymes on t_{mito} , we fixed the activity of one isoenzyme and computed t_{mito} vs. the activity of the other. Figures 7 and 8 demonstrate that the MMCK is able to affect t_{mito} only if the MMCK activity falls below 0.15.

We give the description of the processes that lead to the unimodal behavior of t_{mito} in our model, presented in Figure 6. Since the model has a diffusion barrier between the IMS and the cytosol, the cytosolic ADP and mitochondrial IMS ADP_i may differ considerably. For other metabolites the barrier is not important since their concentrations are considerably higher than those of ADP while their fluxes are of similar order of magnitude. As the MMCK activity is about 6 times higher than MiCK activity in our model, the MMCK reaches its equilibrium earlier for increasing V_{CK} . We split the whole range of V_{CK} into three different regions and describe the modes of signal propagation in each of these.

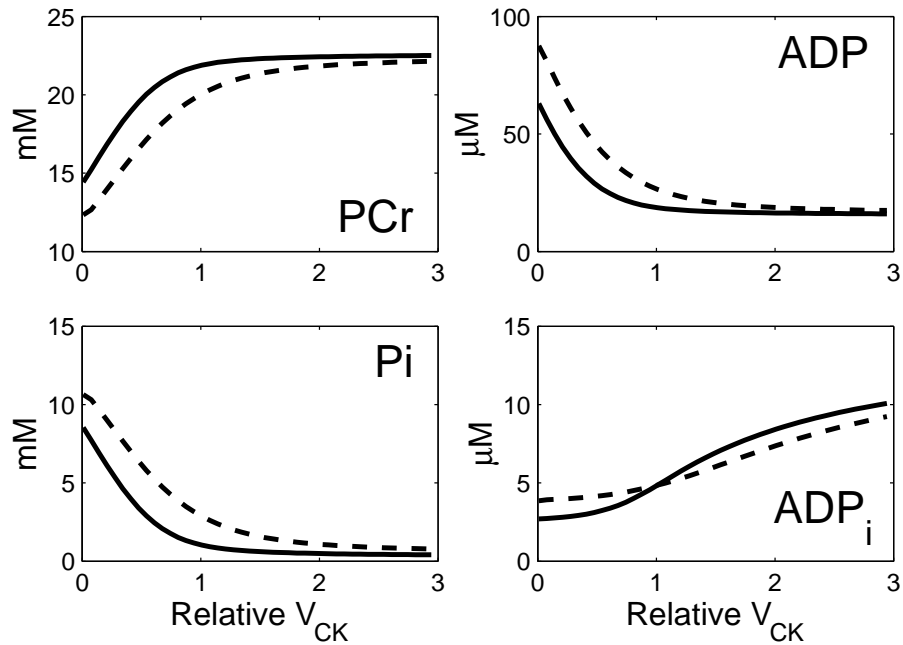


Figure 3: Simulated concentrations of metabolites in cytosol (PCr, Pi, ADP) and in mitochondrial intermembrane space (ADP_i) at baseline (solid lines) and at 40% increased (dashed lines) workloads. Baseline ATP consumption was chosen $500\mu M/s$. ATP concentration remained virtually constant for all V_{CK} (not shown). Relative V_{CK} means that the activities of both MiCK and MMCK are modified proportionally. $V_{CK} = 1$ corresponds to normal rabbit activities of these isoenzymes.

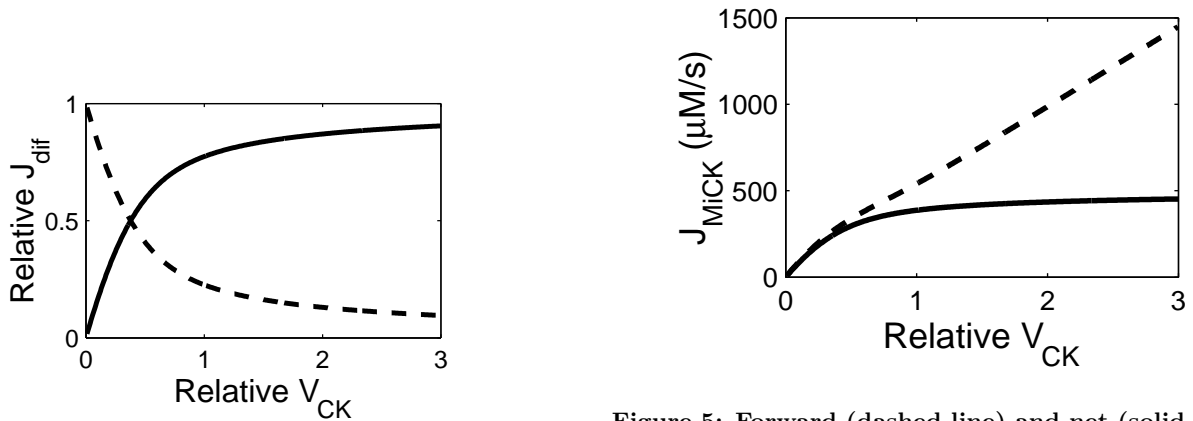


Figure 4: Redistribution of the diffusional flux J_{dif} of ATP (dashed line) and PCr (solid line) from mitochondria depending on CK system activity. Such redistribution demonstrates the activation of the PCr shuttle. This result is for basal workload.

Figure 5: Forward (dashed line) and net (solid line) reaction rates of MiCK isoform. Note that at low V_{CK} , the flux through MiCK is strongly unidirectional, determining the maximal possible activation of PCr shuttle. As MMCK activity is about 6 times higher than that of MiCK, the MMCK reaction is at $V_{CK} = 1$ near equilibrium (not shown). Forward reaction means PCr production. The difference between the dashed and solid lines is the backward flux.

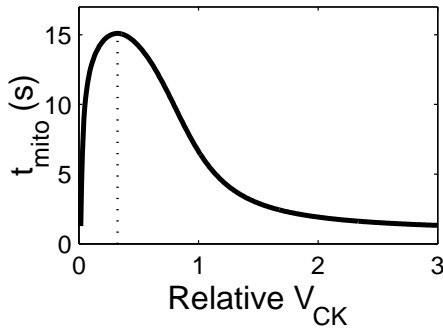


Figure 6: Response times of the mitochondrial respiration after a step change in cytosolic ATP consumption. Note that the peak of t_{mito} at $V_{CK} = 0.33$ (dotted line) coincides well with the notable appearance of the backward flux through MiCK in Figure 5.

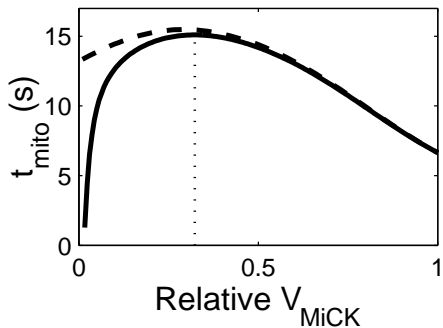


Figure 7: Response times depend on MMCK activity only if also MiCK activity is low. The dashed line shows t_{mito} vs. MiCK activity (V_{MiCK}) for the MMCK activity fixed, $V_{MMCK} = 1$. The curve of response times from Figure 6 (solid line) is given for a comparison, dotted line shows its peak at $V_{MiCK} = 0.33$. Note that the considerable difference between these curves can be observed only for $V_{MiCK} < 0.33$.

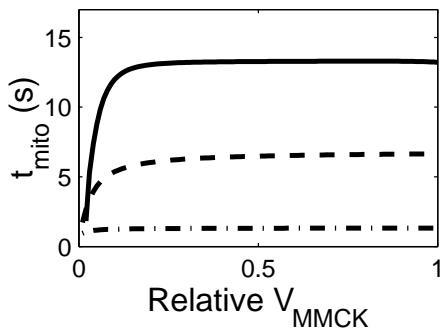


Figure 8: Response times for V_{MiCK} equal to 0, 1, or 3 (solid, dashed, or dashed-dotted lines, resp.) vs. MMCK activity. This is a further demonstration that MMCK can control t_{mito} only at very low V_{CK} values.

- Low CK ($V_{CK} < 0.03$) In this range of V_{CK} , the signal propagates very fast ($t_{mito} < 1s$). This result is obvious, because the step in workload leads to the rapid increase in ADP which is not buffered by CK and propagates therefore rapidly to the IMS and activates mitochondrial ATP synthesis.
- MiCK low, MMCK high ($0.03 < V_{CK} < 0.33$) By gradually activating CK, the signal propagation becomes slower. This slowing occurs in parallel with MMCK approaching its equilibrium and being able to buffer cytosolic ADP. At the same time, the MiCK works virtually unidirectionally controlling the flux through the PCr shuttle. As the shuttle is only partly activated (see Figure 4), most of the energy transfer goes via ADP/ATP. Due to the diffusion barrier, this leads to relatively high cytosolic ADP concentrations inducing, via CK equilibrium, low PCr/Cr ratio and therefore high Pi, which regulates the respiration. As Pi is well above its K_m for mitochondria ($800\mu M$ in the model), the sensitivity of the ATP synthesis to the changes in Pi is low.
- High CK ($V_{CK} > 0.33$). In this mode, the signal propagation becomes faster in parallel with the MiCK approaching its equilibrium. Further activation of MMCK does not affect t_{mito} (Figure 8). As the PCr, Cr, and ATP levels in cytosol do not differ much from their IMS levels, the active MiCK reduces also the difference between ADP and ADP_i by increasing ADP_i. The closer the MiCK to equilibrium, the smaller the difference between ADP and ADP_i and therefore the higher the flux that goes through the PCr shuttle. Increase in ADP_i translates to the decrease in Pi via incorporation of phosphate into PCr to keep the ATP synthesis constant for different V_{CK} values. As Pi becomes lower, the ATP synthesis becomes more sensitive to it resulting in shorter t_{mito} . Interestingly, in this mode ADP_i has negative control over respiration (see Figure 3).

Next we demonstrate the influence of removing the diffusion barrier to t_{mito} . By removing the barrier we mean here its reduction by 10 times for all metabolites diffusing between the IMS and the cytosol. It turns out that this influence is very strong (see Figure 9). The peak of the t_{mito} curve is completely removed. The reason for this is that ADP and ADP_i cannot differ much from each other any more which keeps ADP_i much higher than if the barrier were present. This in turn translates into lower Pi concentrations that control the signal transduction. For $V_{CK} \rightarrow 0$ we observed $Pi \rightarrow 800\mu M$ (results not shown) which is an order of magnitude lower than with the diffusion barrier present (see Figure 3). The removal of the barrier results also in much more stable PCr levels at low V_{CK} and the lack of considerable activation of the PCr shuttle. Only about 20% of the flux of high energy phosphates was carried by the shuttle at $V_{CK} = 3$.

3.3 Comparison with the experiment

Figure 10 shows the effect of graded CK inhibition in isolated perfused rabbit hearts on the mitochondrial oxygen consumption as a response to workload step [10], and the

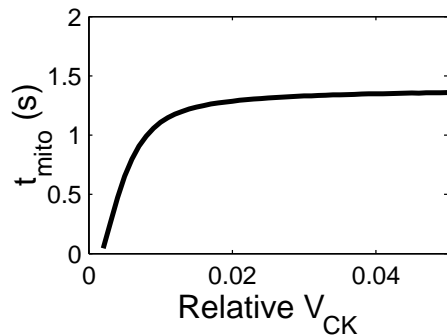


Figure 9: Reduction of the diffusion barrier between the cytosolic and mitochondrial intermembrane space compartments by 10 times reduces strongly t_{mito} removing the peak. See Figure 6 for comparison.

model fit to these experiments. To replicate the experiments, we had to modify some of the model parameters compared to those used in the previous simulations. The modified parameters were: the maximal ATP synthesis rate $V_{synmax} = 1610\mu\text{M/s}$ instead of $4600\mu\text{M/s}$; total phosphate in the system $\text{Pi}_{tot} = 34\text{mM}$ instead of 32mM ; the restriction on outer membrane was 9 times lower than used for most of the simulations above. Also, we used the maximal MiCK and MMCK activities measured by Harrison et al [10] for the t_{mito} experiments 0.35 IU/mgdw and 7.35 IU/mgdw at $T = 25^\circ\text{C}$, respectively. Interestingly, the maximal MiCK activity was about 3 times lower than found by other groups [12] and used in our other simulations. Therefore, the relative $V_{CK} = 100\%$ in Figure 10 is comparable to the $V_{CK} = 0.33$ in Figure 6. Although the model is not able to fit the experiment without modification of some of the model parameters, the model is able to reproduce qualitatively the most important observation made in this experiment — the decrease of t_{mito} as the CK is inhibited.

3.4 Comparison with the results from the extended models

Repeating the simulations shown in this section on a more extensive cardiac cell metabolism model developed previously [24] did not reveal qualitatively different results. Also we repeated the simulations replacing steady ATP hydrolysis rate with pulsating ATP hydrolysis (beating heart); the influence of the pulsation of hydrolysis to t_{mito} was minimal regardless of the considerable oscillations of some metabolites (results not shown).

4. DISCUSSION

In this work we analyzed the mitochondrial response time t_{mito} depending on the relative activity of the CK system using a simple mathematical model, but revealing relatively complex behavior. The model showed the unimodal dependency of t_{mito} on the CK activity (see Figure 6). The left branch demonstrates the qualitative replication of the experimentally observed phenomenon: the decrease of t_{mito} when approaching very low CK activities (Figure 10). However, the right descending branch has not been experimentally observed; this may be due to the low mitochondrial CK

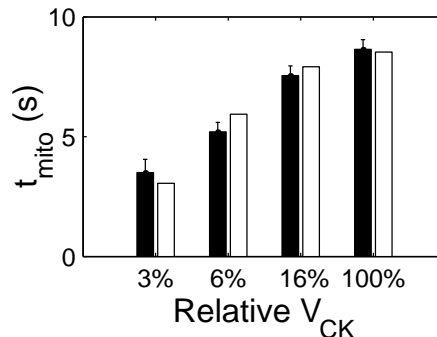


Figure 10: Mitochondrial response times of perfused rabbit hearts to workload steps corresponding to different levels of CK activity (solid bars with $\pm\text{SE}$) and simulation of these experiments (empty bars). Different levels of CK activity in experiments were obtained by infusing different amounts of an irreversible CK inhibitor (iodoacetamide) before the t_{mito} measurements. The CK activities were determined after the experiments. Experimental data from [10].

activity in the rabbit hearts used for the experiments and the lack of animal models with overexpression of CK. The response times on different branches were controlled by the activities of different CK isoenzymes. The unimodal shape of the t_{mito} curve was strongly affected by the strength of the diffusion barrier between the sites of ATP production and consumption; the removal of the barrier removed the peak (unimodality) by reducing the signal buffering capacity of the CK system.

4.1 Adequacy of the model

The model possesses the following important properties that have been experimentally observed by many different groups. First, it is metabolically stable meaning that for low and moderate workloads, the ATP and PCr levels remain practically constant. Second, the energy transfer occurs mostly via the PCr shuttle. Third, at moderate workloads, the PCr level drops when CK is inhibited.

The model was used to simulate the t_{mito} experiments with CK inhibition shown in Figure 10. However, the fit was sensitive to small changes of the parameters and it should be taken only as a qualitative replication of the experimental observations. It is not possible to compare the data in Figure 10 directly with the results presented in other figures, because in this experiment the oxygen consumption (workload) could not be kept the same for all CK levels. Also, the MiCK activity for the control group denoted as 100% of relative V_{CK} in Figure 10 was only about 1/3 of the MiCK activity found in adult rabbit heart by other groups [12, 16] implying the MiCK/MMCK ratio of activities 1/20 in these hearts instead of 1/6.

The lack of glycolysis is perhaps the biggest shortcoming of our model concerning the simulation of mitochondrial response time experiments. Most of these experiments are performed using glucose as a substrate. The workload steps

may induce a short burst of lactate production implying the temporary activation of glycolysis which may delay the signal transduction [23]. If pyruvate was used as a substrate instead of glucose then 1–3s shorter response times were observed [23]. On the other hand, glycolysis seems to cause only a short delay and our simulation results with the current model should be adequate to analyze the effects of CK inhibition qualitatively. We plan to include glycolysis in our model as a next step.

Another property missing in our model is the functional coupling between the MiCK and oxidative phosphorylation. However, this coupling seems to be relevant only at low total adenine nucleotide concentrations. Erickson-Viitanen.et.al [7] have shown that the strength of the coupling was inversely proportional to the ATP level; for ATP=0.7mM, the coupling caused only 3% deviation from the radioactive label incorporation into PCr predicted for reactions without coupling. As in our simulations the ATP levels are above 9mM, the absence of coupling is justified.

In the future it may be necessary to include also the partial parallel activation of mitochondria by calcium to our model to simulate the possible influence of the increased average calcium at higher heart rate after a workload step. Calcium can activate respiration very rapidly: Territo.et.al [22] observed as short response times of isolated mitochondria to calcium addition as 0.27s. Similar mechanism may exist in the intact heart. Such activation may be stronger if there is a calcium overload or an impaired calcium handling. If mitochondria are really activated during a workload step then we expect shorter response times than predicted by our current model. Note that the shortening of t_{mito} by calcium activation may be twofold: in addition to producing more ATP at given ADP and Pi levels, mitochondria become also more sensitive to these metabolites. However, experimental evidence for the rabbit heart model indicates that calcium activation does not play a big role [23] and the model is therefore probably adequate to explain the effects of creatine kinase inhibition.

4.2 How CK isoenzymes determine t_{mito}

Our results show that t_{mito} can be strongly influenced by the activity of the CK system. Without the CK activity present, very short t_{mito} values can be observed, because ADP in the model is not buffered. The MMCK isoform is able to increase t_{mito} by buffering ADP, while its signal buffering capacity can be strongly increased by the diffusion barrier between the sites of ATP production and consumption. In contrast, the MiCK isoform is able to speed up the signal transduction and overcome the influence of the diffusion barrier. The latter occurs via MiCK reaching the equilibrium, which results in relatively low Pi and, therefore, in increased sensitivity of respiration to small Pi changes.

The peak in t_{mito} is completely removed by reducing the diffusion barrier (see Figure 9). The removal of the barrier mimics the situation where the MiCK would reach its equilibrium in parallel with the MMCK (MMCK will establish the equilibrium in the IMS). Our simulations showed that for any V_{CK} , the cytosolic Pi would remain below 1mM if there is no diffusion barrier.

4.3 Diffusion barrier between the energy production and consumption sites

In the model we used a diffusion barrier that induced ADP concentration differences between the cytosol and the IMS of up to 60 μ M at 1/4 of the maximal ATP synthesis rate. The model lost some important properties when the diffusion barrier between the IMS and cytosolic compartments was 10 times reduced. In the latter case, most of the energy left the mitochondria in the form of ATP and the PCr shuttle worked only at very low rate. The inhibition of the CK system caused about an order of magnitude smaller changes of PCr and Pi levels than with the barrier present. Such behavior of the model would be in contradiction with experiments. Dos Santos [6] inhibited the CK system in perfused rabbit hearts to 14% of its original activity and observed an increase of Pi from 1 to 5mM and a drop of PCr from 22 to 14mM which are comparable to those exhibited by our model (see Figure 3). This indicates that the presence of some diffusion barrier between the sites of energy production and consumption may be necessary.

One possible source of the barrier may be the existence of the microcompartment between the MiCK and ANT which is diffusionally separated from the IMS compartment. Interestingly, the strength of this barrier seems to depend inversely on the ATP level [7]. Several groups have proposed that the heart mitochondrial outer membrane permeability is low (see [18] for a review). However, our recent unpublished results show that this barrier, if it exists, can generate ADP concentration differences only up to 20 μ M at half-maximal workloads. It is thought that diffusion through myofibrils cannot cause high diffusion gradients. Many groups have measured the diffusion coefficients of small metabolites in different muscle types [5, 11] and arrived at the conclusion that their diffusion is about 2–3 times slower than in water. This means that at least 1/3 of the cell volume must be free for diffusion. As mitochondria, SR, nuclei and T-tubules occupy about 30% of the heart cell volume, cytosol about 13% and the rest is filled with myofibrils [8], also at least 1/3 of the myofibrillar volume must be free for metabolite diffusion. With such diffusion-free space, only the concentration differences of few μ M can be generated over distances of 1–2 μ m. This conclusion is in accord with the results of the numerical simulation of intracellular ADP gradients in working heart by Vendelin.et.al [24]. The 3D electron microscopic (EM) tomographic reconstructions of the mitochondria of rat liver cells demonstrate that the mitochondria are partly wrapped by endoplasmic reticulum [13]. Using the EM, Sharma.et.al [19] have shown the close proximity of the mitochondria and sarcoplasmic reticulum (SR) in rat heart cells. It is not clear whether the proximity of the SR causes the diffusion limitation. While it may limit the diffusion of metabolites to myofibrils, it contains active ATP consuming sites juxtaposed with mitochondria. In summary, it is not clear how much these factors contribute to the diffusion barrier.

An alternative hypothesis is that glycolytic enzymes and perhaps MMCK interact with the phosphate metabolites being transported between myosin ATPases and ion pumps on the one hand and the mitochondria on the other. Active enzymes may hinder diffusion to and from ATP consuming sites, and may be positioned in such a way that they

do not hinder bulk diffusion. This hypothesis would agree with the idea that glycolytic enzymes and creatine kinase buffer ADP, ATP and Pi and interact intensively with the metabolic signal between sites of ATP consumption and production (review: [23]).

We did our simulations using the CK activities of the rabbit. About 15% of the total CK activity of adult rabbit heart is in the mitochondria [16]. In contrast, adult rat heart can have up to 40% of the CK activity in mitochondria while the total CK activity is comparable to that of rabbit [25]. This may lead to the differences in regulation mechanisms and energy transfer modes in these species. Based on modeling we propose that measuring t_{mito} in perfused rat hearts after a graded inhibition of CK and using pyruvate as a substrate to eliminate the possible interference of glycolysis may let one "probe" the diffusion barrier. If the control rat hearts will show shorter response times than hearts with partly inhibited CK system then the considerable barrier is present and it may be possible to quantitate it.

5. CONCLUSIONS

In this work we analyzed the mitochondrial response time depending on the relative activity of the CK system using a simple mathematical model. We conclude that the buffering role of the CK system is determined by the activity of the myofibrillar CK (MMCK) while the energy transfer role is controlled by the activity of the mitochondrial CK (MiCK). The diffusion barrier between the energy production and consumption sites can strongly increase the signal buffering capacity of CK system. We propose that there may exist differences in regulation mechanisms and energy transfer modes in species with relatively low MiCK activity such as rabbit compared to species with high MiCK activity such as rat. This study demonstrates that developing a model of muscle energy metabolism, let alone a Virtual Muscle Cell, requires extensive testing of the model against experimental data.

6. ACKNOWLEDGEMENTS

This research has been supported by a Marie Curie Fellowship of the European Community programme Improving Human Research Potential and the Socio-economic Knowledge Base under contract number HPMF-CT-1999-00309. It was further supported by an Established Investigator grant from the Netherlands Heart Foundation, number D94.016.

7. REFERENCES

- [1] M. K. Aliev and V. A. Saks. Compartmentalized energy transfer in cardiomyocytes: Use of mathematical modeling for analysis of *in vivo* regulation of respiration. *Biophys. J.*, 73:428–445, 1997.
- [2] S. P. Bessman and P. J. Geiger. Transport of energy in muscle: The phosphocreatine shuttle. *Science*, 211:448–452, 1981.
- [3] B. Chance and G. R. Williams. The respiratory chain and oxidative phosphorylation. *Adv. Enzymol.*, 17:65–134, 1956.
- [4] Y. Chung, R. Sharman, R. Carlsen, S. W. Unger, D. Larson, and T. Jue. Metabolic fluctuation during a muscle contraction cycle. *Am. J. Physiol.*, 274(3 Pt 1):C846–C852, Mar 1998.
- [5] R. A. de Graaf, A. van Kranenburg, and K. Nicolay. In vivo 31P-NMR diffusion spectroscopy of ATP and phosphocreatine in rat skeletal muscle. *Biophys. J.*, 78(4):1657–1664, Apr 2000.
- [6] P. DosSantos. *Controle Bioenergetique de la Fonction Myocardique*. PhD thesis, Universite de Bordeaux 2, 1998.
- [7] S. Erickson-Viitanen, P. Viitanen, P. J. Geiger, W. C. Yang, and S. P. Bessman. Compartmentation of mitochondrial creatine phosphokinase. I. Direct demonstration of compartmentation with the use of labeled precursors. *J. Biol. Chem.*, 257(23):14395–14404, Dec 1982.
- [8] A. M. Gerdes and F. H. Kasten. Morphometric study of endomyocardium and epimyocardium of the left ventricle in adult dogs. *Am. J. Anat.*, 159(4):389–394, Dec 1980.
- [9] B. L. Hamman, J. A. Bittl, W. E. Jacobus, P. D. Allen, R. S. Spencer, R. Tian, and J. S. Ingwall. Inhibition of the creatine kinase reaction decreases the contractile reserve of isolated rat hearts. *Am. J. Physiol.*, 269(3 Pt 2):H1030–H1036, Sep 1995.
- [10] G. J. Harrison, M. H. van Wijhe, B. de Groot, F. J. Dijk, and J. H. van Beek. CK inhibition accelerates transcytosolic energy signaling during rapid workload steps in isolated rabbit hearts. *Am. J. Physiol.*, 276(1 Pt 2):H134–H140, Jan 1999.
- [11] S. T. Kinsey, B. R. Locke, B. Penke, and T. S. Moerland. Diffusional anisotropy is induced by subcellular barriers in skeletal muscle. *NMR Biomed.*, 12(1):1–7, Feb 1999.
- [12] A. V. Kuznetsov and V. A. Saks. Affinity modification of creatine kinase and ATP-ADP translocase in heart mitochondria: determination of their molar stoichiometry. *Biochem. Biophys. Res. Commun.*, 134(1):359–366, Jan 1986.
- [13] C. A. Mannella, K. Buttle, B. K. Rath, and M. Marko. Electron microscopic tomography of rat-liver mitochondria and their interaction with the endoplasmic reticulum. *Biofactors*, 8(3-4):225–228, 1998.
- [14] R. A. Meyer, H. L. Sweeney, and M. J. Kushmerick. A simple analysis of the phosphocreatine shuttle. *Am. J. Physiol.*, 246:C365–C377, May 1984.
- [15] A. M. Mood and F. A. Graybill. *Introduction to the Theory of Statistics*. McGraw-Hill, New York, 2nd edition, 1963.
- [16] S. B. Perry, J. McAuliffe, J. A. Balschi, P. R. Hickey, and J. S. Ingwall. Velocity of the creatine kinase reaction in the neonatal rabbit heart: role of mitochondrial creatine kinase. *Biochemistry*, 27(6):2165–2172, Mar 1988.

- [17] V. A. Saks, G. B. Chernousova, D. E. Gukovsky, V. N. Smirnov, and E. I. Chazov. Studies of energy transport in heart cells. mitochondrial isoenzyme of creatine phosphokinase: Kinetic properties and regulatory action of Mg^{2+} ions. *Eur. J. Biochem.*, 57(1):273–290, Sep 1975.
- [18] V. A. Saks, Z. A. Khuchua, E. V. Vasilyeva, O. Y. Belikova, and A. V. Kuznetsov. Metabolic compartmentation and substrate channeling in muscle cells. *Mol. Cell. Biochem.*, 133/134:155–192, Apr/May 1994.
- [19] V. K. Sharma, V. Ramesh, C. Franzini-Armstrong, and S.-S. Sheu. Transport of Ca^{2+} from sarcoplasmic reticulum to mitochondria in rat ventricular myocytes. *J. Bioenerg. Biomembr.*, 32(1):97–104, 2000.
- [20] H. E. Smith and E. Page. Morphometry of rat heart mitochondrial subcompartments and membranes: application to myocardial cell atrophy after hypophysectomy. *J. Ultrastruct. Res.*, 55(1):31–41, Apr 1976.
- [21] C. D. Stoner and H. D. Sirak. Steady-state kinetics of the overall oxidative phosphorylation reaction in heart mitochondria. *J. Bioenerg. Biomembr.*, 11(5-6):113–146, Dec 1979.
- [22] P. R. Territo, S. A. French, M. C. Dunleavy, F. J. Evans, and R. S. Balaban. Calcium activation of heart mitochondrial oxidative phosphorylation: rapid kinetics of mVO_2 , NADH, and light scattering. *J. Biol. Chem.*, 276(4):2586–2599, Jan 2001.
- [23] J. H. G. M. van Beek, X. Tian, C. J. Zuurbier, B. de Groot, C. J. A. van Echteld, and M. H. J. Eijgelshoven. The dynamic regulation of myocardial oxidative phosphorylation: Analysis of the response time of oxygen consumption. *Mol. Cell. Biochem.*, 184:321–344, 1998.
- [24] M. Vendelin, O. Kongas, and V. Saks. Regulation of mitochondrial respiration in heart cells analyzed by reaction-diffusion model of energy transfer. *Am. J. Physiol.*, 278(4):C747–C764, Apr 2000.
- [25] R. Zahler and J. S. Ingwall. Estimation of heart mitochondrial creatine kinase flux using magnetization transfer NMR spectroscopy. *Am. J. Physiol.*, 262(4 Pt 2):H1022–H1028, Apr 1992.
- [26] S. D. Zimmer, K. Ugurbil, S. P. Michurski, P. Mohanakrishnan, V. K. Ulstad, J. E. Foker, and A. H. From. Alterations in oxidative function and respiratory regulation in the post-ischemic myocardium. *J. Biol. Chem.*, 264(21):12402–12411, Jul 1989.

APPENDIX

Here we describe the model used for our simulations. The model consists of two compartments, the cytosol and the intermembrane space (IMS). In both compartments the following metabolites are considered: ATP, ADP, PCr, Cr, and Pi. The compartments are separated by a partly permeable

diffusion barrier. In the IMS compartment the ATP synthesis and MiCK reactions are considered, in the cytosolic compartment the MMCK reaction and ATP hydrolysis occur. The parameters used in modeling are given in Table 1.

The rate equations for all metabolites are as follows. The subscript i denotes the IMS concentrations, the cytosolic ones are without subscript.

$$A\dot{T}P = (-V_{hyd} - V_{MMCK} + J_{ATP})/V_{cyt}, \quad (1)$$

$$A\dot{D}P = (V_{hyd} + V_{MMCK} + J_{ADP})/V_{cyt}, \quad (2)$$

$$P\dot{C}r = (V_{MMCK} + J_{PCr})/V_{cyt}, \quad (3)$$

$$\dot{C}r = (-V_{MMCK} + J_{Cr})/V_{cyt}, \quad (4)$$

$$\dot{P}i = (V_{hyd} + J_{Pi})/V_{cyt}, \quad (5)$$

$$A\dot{T}P = (-V_{hyd} - V_{MiCK} - J_{ATP})/V_{ims}, \quad (6)$$

$$A\dot{D}P = (V_{hyd} + V_{MiCK} - J_{ADP})/V_{ims}, \quad (7)$$

$$P\dot{C}r = (V_{MiCK} - J_{PCr})/V_{ims}, \quad (8)$$

$$\dot{C}r = (-V_{MiCK} - J_{Cr})/V_{ims}, \quad (9)$$

$$\dot{P}i = (V_{hyd} - J_{Pi})/V_{ims}, \quad (10)$$

where V_{syn} , V_{hyd} , V_{MMCK} , and V_{MiCK} are the reaction rates per volume of intracellular diffusion-free water, J_{Met} are the diffusion fluxes between the compartments (Met denoting any of the metabolites involved), and V_{ims} and V_{cyt} are the fractional volumes of the cytosolic and IMS compartments, respectively, with respect to total diffusion-free cell volume.

The CK reaction rate v_{CK} is described by the equation [17],

$$V_{CK} = \left(V_f \frac{ATP \cdot Cr}{K_{ia}K_b} - V_b \frac{ADP \cdot PCr}{K_{ic}K_d} \right) / Den_{CK}, \quad (11)$$

where

$$Den_{CK} = 1 + \frac{Cr}{K_{ib}} + \frac{PCr}{K_{id}} + ATP \left(\frac{1}{K_{ia}} + \frac{Cr}{K_{ia}K_b} \right) + ADP \left(\frac{1}{K_{ic}} + \frac{PCr}{K_{id}K_c} + \frac{Cr}{K_{ic}K_{Ib}} \right). \quad (12)$$

The equations (11) and (12) govern the rates of both V_{MiCK} and V_{MMCK} when the concentrations of the corresponding compartment and the kinetic constants for the appropriate isoenzyme from Table 1 are plugged in.

The ATP synthesis rate is a Michaelis-Menten-type equation depending only on ADP_i and Pi_i [21].

$$V_{syn} = V_{synmax} \frac{ADP_i \cdot Pi_i}{K_{Pi} \cdot K_{ADP} \cdot Den_{syn}}, \quad (13)$$

where

$$Den_{syn} = 1 + \frac{ADP_i}{K_{ADP}} + \frac{Pi_i}{K_{Pi}} + \frac{ADP_i \cdot Pi_i}{K_{ADP} \cdot K_{Pi}}. \quad (14)$$

Diffusional fluxes between the compartments are as follows.

$$J_{ATP} = R_{ATP}(ATP_i - ATP), \quad (15)$$

$$J_{ADP} = R_{ADP}(ADP_i - ADP), \quad (16)$$

$$J_{PCr} = R_{PCr}(PCr_i - PCr), \quad (17)$$

$$J_{Cr} = R_{Cr}(Cr_i - Cr), \quad (18)$$

$$J_{Pi} = R_{Pi}(Pi_i - Pi), \quad (19)$$

where R_{Met} is the permeability for the metabolite Met . Positive direction of flux is from the IMS to cytosol.

The metabolites obey the following moieties conservations

$$(ATP + ADP)V_{cyt} + (ATP_i + ADP_i)V_{ims} = AdN_{tot}(V_{cyt} + V_{ims}), \quad (20)$$

$$(PCr + Cr)V_{cyt} + (PCr_i + Cr_i)V_{ims} = Cr_{tot}(V_{cyt} + V_{ims}), \quad (21)$$

$$(ATP + PCr + Pi)V_{cyt} + (ATP_i + PCr_i + Pi_i)V_{ims} = Pi_{tot}(V_{cyt} + V_{ims}). \quad (22)$$

Table 1: Parameters of the model. Our model simulates reactions occurring at $T = 37^\circ\text{C}$. To convert the experimentally measured rates, determined at $T = 25^\circ\text{C}$, the temperature coefficient $Q_{10} = 2$ was used.

| Parameter | Value | Reference |
|---------------------------|----------------------------------|-------------------|
| MiCK | | |
| V_f (PCr production) | $2.658 \cdot 10^3 \mu\text{M/s}$ | [1] ^a |
| V_b (ATP production) | $1.116 \cdot 10^4 \mu\text{M/s}$ | [12] ^b |
| K_{ia} | $7.5 \cdot 10^2 \mu\text{M}$ | [1] |
| K_b | $5.2 \cdot 10^3 \mu\text{M}$ | " |
| K_{ic} | $2.048 \cdot 10^2 \mu\text{M}$ | " |
| K_d | $5.0 \cdot 10^2 \mu\text{M}$ | " |
| K_{ib} | $2.88 \cdot 10^4 \mu\text{M}$ | " |
| K_{id} | $1.6 \cdot 10^3 \mu\text{M}$ | " |
| K_c | $K_{ic}K_d/K_{id}$ | " |
| K_{Ib} | K_{ib} | " |
| MMCK | | |
| V_f (PCr production) | $6.966 \cdot 10^3 \mu\text{M/s}$ | [16] ^c |
| V_b (ATP production) | $2.925 \cdot 10^4 \mu\text{M/s}$ | " ^c |
| K_{ia} | $9.0 \cdot 10^2 \mu\text{M}$ | [1] |
| K_b | $1.55 \cdot 10^4 \mu\text{M}$ | " |
| K_{ic} | $2.224 \cdot 10^2 \mu\text{M}$ | " |
| K_d | $1.67 \cdot 10^3 \mu\text{M}$ | " |
| K_{ib} | $3.49 \cdot 10^4 \mu\text{M}$ | " |
| K_{id} | $4.73 \cdot 10^3 \mu\text{M}$ | " |
| K_c | $K_{ic}K_d/K_{id}$ | " |
| K_{Ib} | K_{ib} | " |
| ATP synthesis | | |
| V_{synmax} | $4.6 \cdot 10^3 \mu\text{M/s}$ | [26] ^d |
| K_{ADP} | $8.0 \cdot 10^2 \mu\text{M}$ | [21] |
| K_{Pi} | $20.0 \mu\text{M}$ | [3] |
| ATP hydrolysis | | |
| V_{hyd} | $4.6 \cdot 10^3 \mu\text{M/s}$ | - |
| Permeabilities | | |
| R_{ATP} | 8.16 s^{-1} | - ^e |
| R_{ADP} | 8.16 s^{-1} | - |
| R_{PCr} | 14.6 s^{-1} | - |
| R_{Cr} | 14.6 s^{-1} | - |
| R_{Pi} | 18.4 s^{-1} | - |
| Fractional volumes | | |
| V_{cyt} | $3/4$ | [20] ^f |
| V_{ims} | $1/16$ | " |
| Total contents | | |
| AdN_{tot} | $9.7 \cdot 10^3 \mu\text{M}$ | - |
| Cr_{tot} | $2.6 \cdot 10^4 \mu\text{M}$ | - |
| Pi_{tot} | $3.2 \cdot 10^4 \mu\text{M}$ | - |

^a $V_b/V_f = 4.199$, according to [1]

^b $3.0 \text{ IU} / \text{mg mito prot}$ at $T = 25^\circ\text{C}$.

^c Calculated from MiCK activity which is about 15% of total CK activity in heart [16].

^d Corresponds to $120 \mu\text{mol}/(\text{gdw} \cdot \text{min})$ of O_2 consumption at $T = 37^\circ\text{C}$.

^e Ratios of the permeabilities are the same as ratios of the diffusion coefficients of these metabolites in muscle [14].

^f Total volume 1 corresponds to $0.615 \text{ mL}/\text{gww}$.